

THERMAL DISTORTION ANALYSES OF A THREE-METER INFLATABLE REFLECTARRAY ANTENNA

Houfei Fang, Michael Lou, John Huang
Jet Propulsion Laboratory
California Institute of Technology
Pasadena, California

Ubaldo Quijano and Lih-Ming Hsia
Department of Mechanical Engineering
California State University at Los Angeles
Los Angeles, California

Abstract

Gossamer space structures are relatively large, flimsy, and lightweight. As a result, they are more easily affected or degraded by space thermal environments compared to other space structures. This study examines the structural integrity of a Three-Meter Ka-Band Inflatable/Self-Rigidizable Reflectarray Antenna under space thermal environments. Space thermal environments discussed by this paper include Earth, Mars, and Jupiter orbits. The most critical structural components of this antenna are the two Spring Tape Reinforced Aluminum Laminate Inflatable/Self-Rigidizable Booms. The effects of the thermal distortion of the booms to surface deviation of the Radio Frequency membrane are also investigated.

1. Introduction

An inflatable/self-rigidizable structural system for a three-meter Ka-band reflectarray antenna has been developed at the Jet Propulsion Laboratory (JPL) in the last several years¹. Figure 1 shows an engineering model recently built for this antenna. The radio frequency (RF) component of this antenna is a flat membrane reflectarray with a large number of copper patches that are illuminated by an offset feed horn. The RF membrane is supported by a rectangular planar frame that consists of two parallel inflatable booms. For stowage of the antenna, the booms can be flattened and rolled up on two mandrels

while the RF membrane is rolled up on a composite cylinder that connects the mandrels. After the stowed antenna is launched into space, it will be deployed by inflation, i.e., by allowing pressurized gas to flow into the booms. The dynamics of the deploying booms is controlled by a deployment control device, such as Velcro strips, which are axially attached to the outer surface of the booms. Compared to the mechanically deployable antennas, this inflatable antenna offers a larger aperture with much lower mass and higher package efficiency.

The inflatable booms selected for this particular antenna application are the self-rigidizable Spring-Tape-Reinforced aluminum laminate booms (or simply STR booms) that were also developed at JPL². Figure 2 shows the photo of the end view of two STR booms. The basic construction of a STR boom consists of a thin-walled tube made of aluminum laminate. Four spring tapes are attached to the inside wall of the tube in the axial direction. At this time, commercially available stainless steel measuring tapes, (commonly known as carpenter tapes) are used and we plan to replace them in the future with tapes made of more advanced materials, such as Titanium or carbon-fiber composites. With a wall thickness less than 0.1 mm, a STR boom can be easily flattened, rolled-up (or folded-up), and deployed by a relatively low inflation pressure. Due mainly to the high modulus of elasticity and curved cross-sectional profile of the spring tapes, a STR boom is very strong to resist axial compress load.

This inflatable/self-rigidizable reflectarray antenna belongs to the category of Gossamer space structures. Gossamer space structures are relatively large, flimsy, and lightweight. As a result, they are more easily affected or degraded

Copyright © 2002 by the American Institute of Aeronautics and Astronautics, Inc. The U.S. Government has a royalty-free license to exercise all rights under the copyright claimed herein for governmental purpose. All other rights are reserved by the copyright owner.

by the space thermal environments compared to other space structures. The space thermal environments can cause a space structure to become unstable³ and dimensionally inaccurate^{4,5}. It can also introduce undesired vibrations⁶. Therefore, the effects of thermal loads to this antenna need to be thoroughly studied.

The two STR booms are the most critical components of the three-meter inflatable reflectarray antenna structural system. After the antenna is deployed in space, these booms are under axial compression loads all the time in reaction of the tensioning of the RF membrane. Any thermal loads caused by temperature changes of the booms will be superimposed to the axial compression loads. Since these booms need to be tightly rolled up on mandrels and they have deployment-controlling Velcro strips attached on their surfaces, it is not feasible to use thermal blankets to protect these booms from being exposed to in-space thermal cycling and temperature extremes. To address this issue, thermal distortion analyses are conducted to investigate the effects of in-space thermal disturbances on the structural integrity of the antenna, including buckling capability of the booms, when it is subjected to the Earth orbit as well as deep space thermal environments⁷. Deviation of the RF membrane is also calculated based on the results of the thermal distortion analysis. Details of these two aspects are discussed in the following sections.

2. Buckling strength of a boom with thermal distortion—Earth orbit

During the development of the subjected antenna, the buckling strength of the STR aluminum laminate boom has been analyzed and tested. However, these earlier analyses and test efforts were carried out assuming the booms are perfectly straight. In space the thermal loads will in some cases only heat up one side of a boom and lead to severe bending of the boom. The buckling strength of a bended boom is significantly lower. In order to ensure that the boom is suitable for space applications, its buckling strength under thermal loads must be investigated. The buckling analysis of a STR aluminum laminate boom with thermal distortions can be carried out in three major steps. The first step is to obtain the temperature distribution of a boom under the Earth orbit's thermal condition. The second step is to

analyze the deflection of the boom based on the temperature distribution obtained in step one. The third step is to calculate the buckling capability of the boom with the thermal deflection.

2.1 Temperature Distribution Analysis

Figure 3 is the cross-sectional view of a STR aluminum laminate boom. The outside diameter of the boom is 0.0762 m. The aluminum laminate is composed of one-layer of soft aluminum sandwiched by two-layers of Kapton. The Kapton layers have a thickness of 0.000254 m and the aluminum layer has a thickness of 0.000762 m. The steel carpenter blades have a thickness of 0.000127 m and a width of 0.0254 m. A finite element model was first established to analyze the temperature distribution by using the NASTRAN computer code. In order to capture the temperature differences in the radial direction, solid elements were used in this finite element model. To simulate the steel carpenter tapes, 840 solid elements were used. To simulate the Kapton, 3360 solid elements were used. To simulate the aluminum, 1680 solid elements were used.

For the temperature analysis, the heat flux from the sun, the internal and external radiations of the boom's surfaces, and the conductivities of the materials that make up the boom were taken into consideration. Table 1 displays the properties used in this finite element model for each material. Figure 4 illustrates an isometric view of half the length of the 3.5 meters long model.

Figure 5 shows a cross-sectional view of the finite element model with a 1367.5 W/m^2 heat flux⁸ from the sun being applied to all the top half elements of the outer Kapton layer. The heat flux is applied vertically down.

Figure 6 shows a cross-sectional view of the finite element model with the radiating conditions being applied to the model. The outer layer Kapton and the inner layer Kapton both have an emissivity of 0.7 and the carpenter blades have an emissivity of 0.11.

Figures 7 and 8 show the results of the temperature distribution. Figure 7 is an isometric view of the full-length boom. Figure 8 is a close-up view of the boom. The change in

temperature from the hottest element to the coolest element is 37.53 K.

2.2 Deformation Analysis

This step is to analyze the deformation of the boom under the distributed temperature load calculated by the previous step. All the nodes on the finite element model were loaded with their respective temperatures. Figure 9 is a close-up cross-sectional view of the junction of seven elements showing the temperature loads on five nodes.

A static analysis with the temperature loads was conducted subsequently to acquire the deflection. Figure 10 shows the thermal deflection of the boom.

2.3 Buckling Analysis

The third step, buckling analysis, comes after the deformation analysis. This step is to analyze the buckling strength of the thermally deflected boom. A new finite element model of the curved boom, which is composed of laminate and plate elements, was created to perform the buckling analysis. This new model has 3386 elements and 3444 nodes. To simulate the aluminum and Kapton sections of the boom, 1692 plate elements were used. To simulate the Kapton, carpenter steel blades, and aluminum sections of the boom, 1692 laminate elements were used. And two rigid elements were used to simulate the end caps. Figure 11 shows the side view of this new FEM model.

For the buckling analysis, pin-pin boundary conditions were applied to the centers of two end caps. Figure 12 gives the buckling failure shape of the curved boom. It is calculated that the axial buckling load of the curved boom is 916 N.

It can be concluded from this analysis that the STR aluminum laminate boom of current configuration is able to take 916 N axial buckling load with the Earth orbit's thermal disturbance. As a result, this boom is able to take the designed axial load, which is 156 N¹.

3. RF membrane deviation analysis—Earth orbit

Another aspect of in-space thermal disturbances is the deviation of the RF membrane. Inflatable

booms deflect under the combined mechanical and thermal loads. This boom deflection will, in turn, deviate the orientation of the RF membrane. The deviation of the membrane surface impacts the RF performance of the antenna. Therefore, the deviation of the RF membrane needs to be analyzed also.

It is identified to be the worst situation when the RF surface faces the Sun, because this antenna orientation gives the lowest structural bending stiffness with respect to the temperature loads. The RF membrane deviation analysis has four major steps. The first and second steps are Temperature Distribution analysis and Boom Deformation Analysis (under the thermal loads), which have been presented by sections 2.1 and 2.2. As has been discussed, the STR aluminum booms are axially loaded by the membrane. The third step is to analyze the deformation of booms introduced by the membrane tensioning force and superimposes this deformation on to the thermal deformation. A finite element model was established to analyze the deformations of booms and the deviation of the membrane. Because the membrane does not directly connect to inflatable booms, the membrane is still a flat surface while the boom is bended as shown in Figure 13. The deviation of the membrane is that the surface turns an angle with respect to the bottom line. This angle is called the tilt angle by RF engineers and is very critical for the antenna performance. Figure 14 is the profile view of the deviation of the membrane. The tilt angle is defined as the angle between the membrane and the vertical line.

The tilt angle is caused by two loads, the first one is the temperature load and the second one is the membrane pretensioning force. The angle introduced by temperature load is calculated to be 0.01219 radian (0.698 degree) and the angle introduced by membrane tensioning load is calculated to be 0.00104 radian (0.060 degree). Due to the reason that both angles introduced by temperature load and membrane tensioning load are considerably small, they can be superimposed to be the tilt angle and the tilt angle is then calculated to be 0.01323 radian (0.758 degree).

Unfortunately, this tilt angle is three times bigger than the beam-width, which is 0.22 degree⁹, of the antenna. This large tilt angle significantly degrades the antenna performance. However,

there are several ways to minimize it. The tilt angle is mainly caused by the uneven thermal expansion of the booms. Therefore, using composite material with very low Coefficient of Thermal Expansion (CTE) to replace the current metallic spring tapes (indicated in figure 2) can significantly reduce the thermal bending. On the other hand, spring tapes composed of composite material are much lighter than current steel spring tapes. In order to investigate the result of using composite spring tape to replace the current steel spring tape, a finite element model with carbon fiber spring tape has been developed and analyzed for the thermal distortion. The tilt angle introduced by thermal distortion is calculated to be 0.00155 radian (0.089 degree).

Other methods that can be employed to resolve this large tilt angle problem include mechanically adapting the feed position to the membrane as well as electronically feed adapting by using array of feeds with phase compensation technique. However, using composite spring tape to replace the metallic spring tape is the most feasible and inexpensive method.

4. RF membrane deviation analyses—deep space

This antenna is developed also for deep space applications. In order to study the applicability of this antenna to deep space applications, thermally introduced tilt angles are calculated for Mars orbit and Jupiter orbit with current steel spring tapes and future carbon composite spring tapes. The heat flux for Mar's orbit¹⁰ is 589 W/m² and the heat flux for Jupiter's orbit¹¹ is 51 W/m². The analysis procedure is the same as that has been discussed in section 3. Table 2 gives thermally introduced tilt angles for Earth, Mars, and Jupiter applications. The spring tape material for this table is steel. Table 3 shows thermally introduced tilt angles for Earth, Mars, and Jupiter applications with carbon spring tapes. Results of the Earth orbit are also included in these two tables for reference. The RF performances are discussed based on thermally introduced tilt angles only. The tilt angles introduced by membrane tensioning forces are relatively small and are neglected.

5. Concluding Remarks

A three-meter Ka-band inflatable/self-rigidizable reflectarray antenna has been developed in the

last several years. The most critical structural components of this antenna are two STR aluminum laminate inflatable/self-rigidizable booms. Due mainly to the need of attaching deployment-controlling Velcro strips on their surfaces, these two booms cannot be thermally protected with thermal blankets and will undergo thermal distortions in space. This paper presented results of a study on structural integrity of these booms under space thermal environments, as well as the effects of thermal distortion of the booms to surface deviation of the RF membrane.

The in-space structural integrity of these booms is first investigated. After in-space deployment of the antenna, the two STR booms are continuously loaded by axial forces that react to the tension in the RF membrane. The two booms will also bow due to the circumferentially uneven thermal expansions. This leads to significantly reductions of the buckling capabilities of the booms. The Earth orbit's thermal load condition was used to calculate the temperature distributions and gradients of the boom. The bending of the boom introduced by temperature gradients was determined consequently. Buckling capability of the bended boom was subsequently calculated to be 916 N. The baseline STR boom is capable to take the required load, which is 156 N. Since the Earth application has the most severe thermal environment among all near-term mission applications, it was concluded that the STR booms with current design and configuration is structurally strong enough for both Earth and deep-space applications.

The thermally introduced deviation of the RF membrane is also investigated by this study. The case in which the antenna membrane aperture directly faces the sun is identified as the worst situation because at that moment the inflatable antenna structure has the least moment of inertia to resist the thermal loads. During a typical Earth mission, the RF membrane deviations of the antenna equipped with baseline STR booms was first analyzed. The membrane tilt angle is calculated to be 0.758 degree, which is three times larger than the antenna beam-width (0.22 degree). This large tilt angle will lead to unacceptable degradation of RF performance and must be reduced. There are several ways to remedy this undesirable situation, including: 1) replacing steel spring tapes of the boom with composite

spring tapes, 2) mechanically adapting the feed position to the membrane, and 3) electronically feed adapting by using array of feeds with phase compensation technique. However, replacing steel spring tapes of the boom with composite spring tapes is the most feasible and simplest way. To validate this, two antennas, one with the baseline STR booms and the other with booms that have their steel spring tapes replaced by composite tapes were analyzed for thermal environments of the Earth, Mars, and Jupiter orbits. It is concluded from the results of these analysis that the current booms is not acceptable for Earth missions, but is acceptable for Mars and Jupiter missions. On the other hand, the boom design with composite spring tapes is acceptable for all Earth, Mars, and Jupiter missions.

6. Acknowledgements

The authors wish to thank Mr. Robert Miyake of the Jet Propulsion Laboratory for his advices and comments related to space thermal environments.

The work described in this paper was performed at the Jet Propulsion Laboratory, California Institute of Technology under contract with the National Aeronautics and Space Administration of United States.

7. References

- [1] Houfei Fang, Michael Lou, John Huang, Lih-Min Hsia, and Grigor Kerdanyan, "An Inflatable/Rigidizable Ka-Band Reflectarray Antenna", AIAA 2002-1706, 43rd AIAA/ASME/ASCE/AHS/ASC Structures, Structural Dynamics, and Materials Conference and Exhibit, Denver, Colorado, 22-25 April 2002.
- [2] Michael Lou, Houfei Fang, and Lih-Min Hsia, "Self- Rigidizable Space Inflatable Boom", AIAA Journal of Spacecraft and Rockets, Vol. 39, No.5, pp. 682-690, 2002
- [3] Radu Udrescu, "Nonlinear Thermoelastic Stress Analysis of Panels Exposed to High-Speed Flow Effects", AIAA 2002-1690, 43rd AIAA/ASME/ASCE/AHS/ASC Structures, Structural Dynamics, and Materials Conference and Exhibit, Denver, Colorado, 22-25 April 2002.
- [4] Ahmed K. Noor, James H. Starnes, and Jeanne M. Peters, "Thermomechanical

Response Variability of Composite Panels with Continuous and Terminated Stiffeners", AIAA 2002-1518, 43rd AIAA/ASME/ASCE/AHS/ASC Structures, Structural Dynamics, and Materials Conference and Exhibit, Denver, Colorado, 22-25 April 2002.

[5] Donald J. Davis and Gregory S. Agnes, "Environmental Disturbance Modeling for Inflatable Space Structures", AIAA 2002-1266, 43rd AIAA/ASME/ASCE/ AHS/ASC Structures, Structural Dynamics, and Materials Conference and Exhibit, Denver, Colorado, 22-25 April 2002.

[6] Kyung-Eun Ko and Ji-Hwan Kim, "Thermally Introduced Vibrations of Spinning Composite Structures", AIAA 2002-1623, 43rd AIAA/ASME/ASCE/AHS/ASC Structures, Structural Dynamics, and Materials Conference and Exhibit, Denver, Colorado, 22-25 April 2002.

[7] David G. Gilmore, "Satellite Thermal Control Handbook", The Aerospace Corporation Press, 1994

[8] <http://www.tak2000.com/data/planets/earth.htm>

[9] J. Huang, V. Alfonso Ferial, and H. Fang, "Improvement of the three-meter Ka-band inflatable reflectarray antenna", presented at IEEE Antennas & Propagation Symposium, AP-S/URSI, Boston, MA, July 2001

[10] <http://www.tak2000.com/data/planets/mars.htm>

[11] <http://www.tak2000.com/data/planets/jupiter.htm>

[12] <http://www.matweb.com/SpecificMaterial.asp?bassnum=PDUK01>

[13] Ferdinand P. Beer and Russell Johnston, Jr., "Mechanics of Materials", McGraw Hill, Inc, 1992.

[14] <http://www.matweb.com/SpecificMaterial.asp?bassnum=Q302AA>

[15] <http://161.34.11.100/servlet/EnterpriseMvision/>

[16] Frank P. Incropera and David P. DeWitt, "Introduction to Heat Transfer", John Wiley & Sons, Inc., 1996.

Table 1. Properties used on finite element model

		Kapton ¹²	Aluminum ¹³	Stainless Steel ¹⁴	Carbon Fiber ¹⁵
1	Youngs Modulus (GPa)	2.8	68	193	393
2	Shear Modulus (GPa)		25	77.2	
3	Poisson's Ratio	0.34			0.34
4	Thermal Expansion Coefficient (m/mK)	2.00E-05	2.40E-05	1.72E-05	-0.72E-06
5	Thermal Conductivity (W/mK)	0.12	210	16.2	69.23
6	Specific Heat (J/kgK)	1090	900	500	1090
7	Emmissivity	0.70	0.03	0.11	0.86
8	Absorptivity	0.35	0.16	0.42	0.50
9	Density (kg/m ³)	1420	2700	7860	1810

5.67E⁻⁸ W/m²K⁴ is the value of the Stefan-Boltzmann constant used in the model¹⁶.

Table 2. Thermally introduced tilt angles, steel spring tapes

Orbit	Tilt angle	RF performance
Earth	0.01219 rad. (0.698 deg.)	Poor
Mars	0.00580 rad. (0.332 deg.)	Acceptable
Jupiter	0.00054 rad. (0.031 deg.)	Good

Table 3. Thermally introduced tilt angles, carbon spring tapes

Orbit	Tilt angle	RF performance
Earth	0.00155 rad. (0.089 deg.)	Good
Mars	0.00120 rad. (0.069 deg.)	Excellent
Jupiter	0.00011 rad. (0.006 deg.)	Excellent

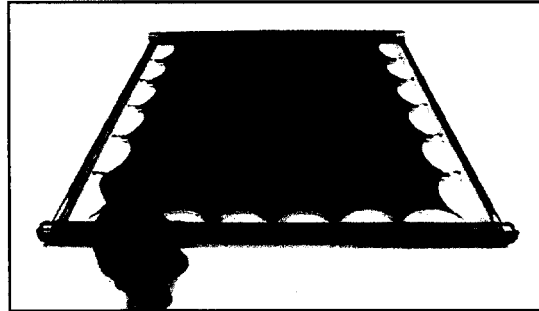


Figure 1. Three-meter inflatable/self-rigidizable reflectarray antenna

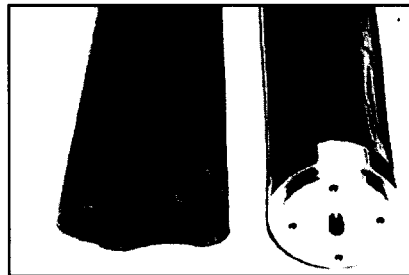


Figure 2. Photo of the STR boom's end view

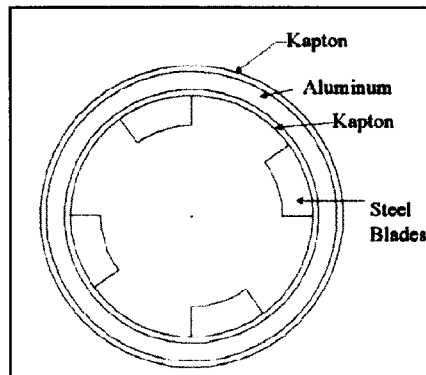


Figure 3. Schematic of the cross-section of a STR aluminum laminate boom

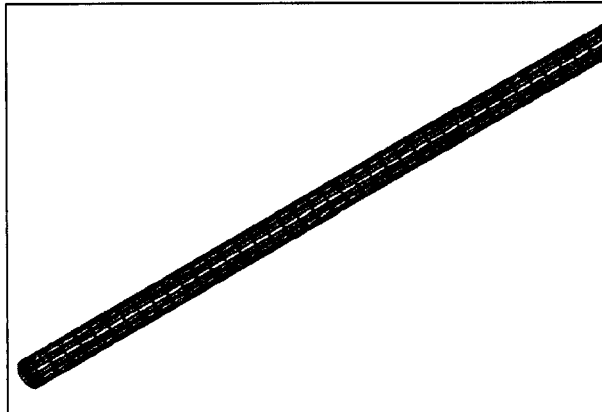


Figure 4. Finite element model of the 3.5 meters boom

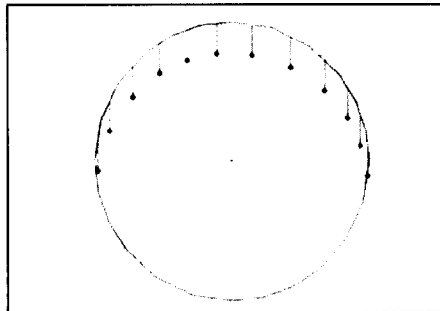


Figure 5. Application of heat flux on finite element model

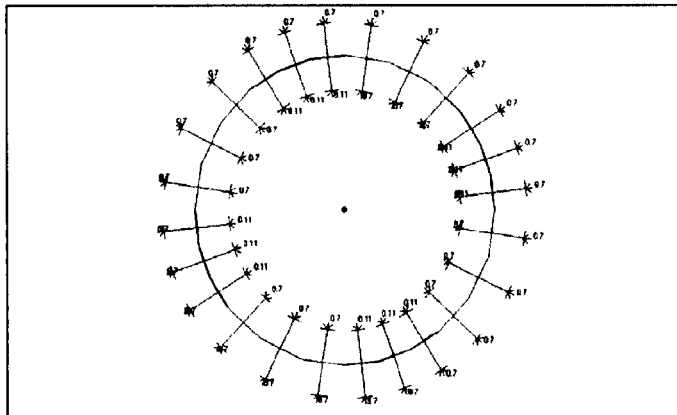


Figure 6. Application of radiating conditions on finite element model

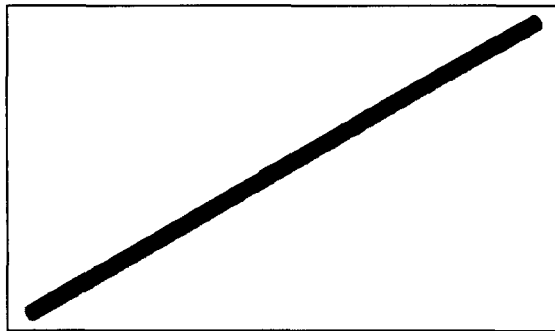


Figure 7. Temperature distribution of a 3.5 meters boom

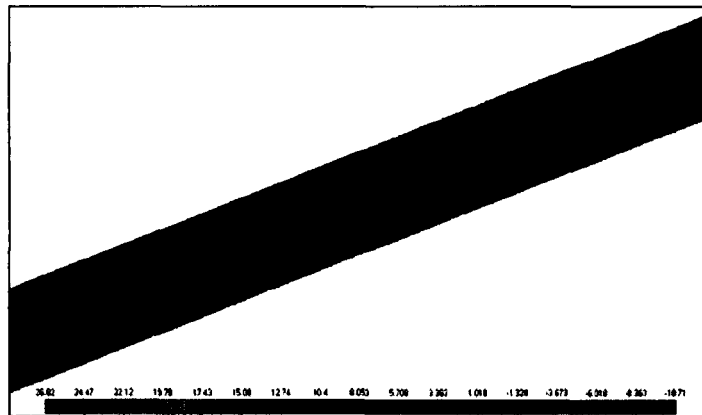


Figure 8. Close view of the temperature distribution of a 3.5 meters boom

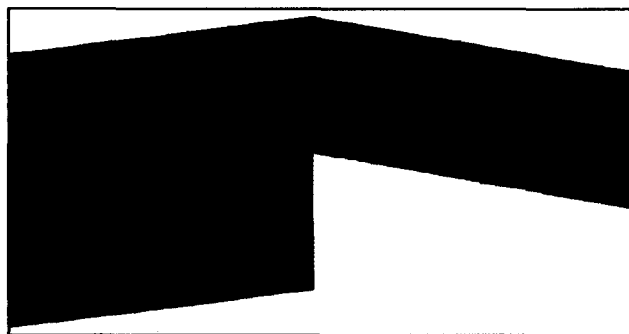


Figure 9. Temperature loading on nodes

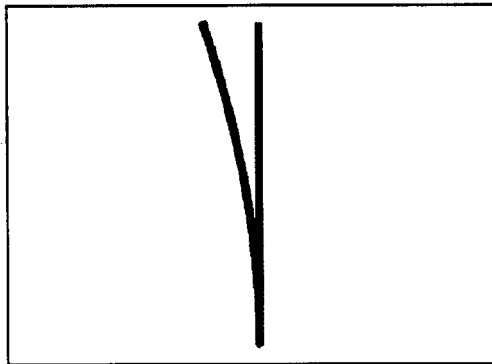


Figure 10. Deflection of the boom

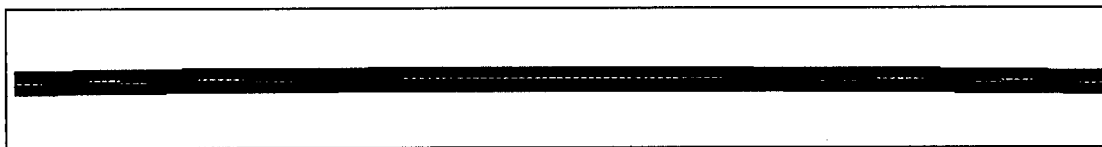


Figure 11. FEM model of a curved boom

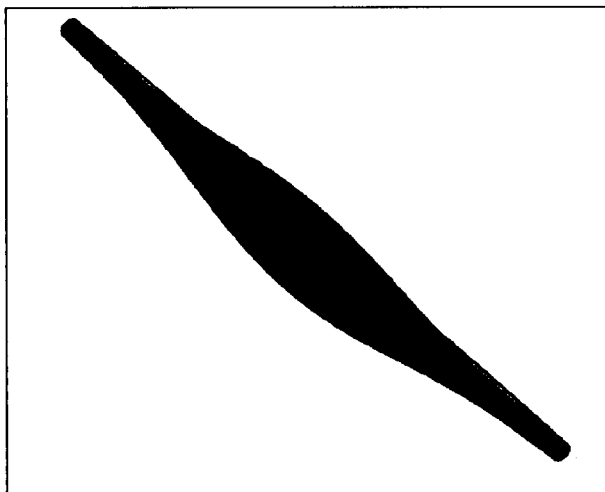


Figure 12. Buckling failure shape of the curved boom

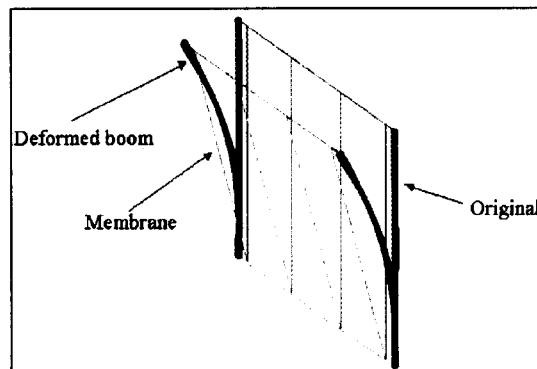


Figure 13. Bending of the booms and turning of the membrane

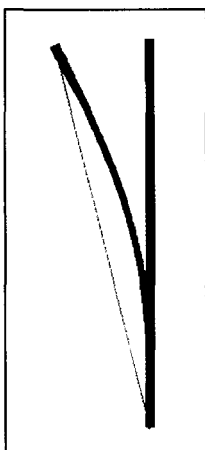


Figure 14. Profile view of the membrane deviation